

# Identification of enhancer of mRNA decapping 4 as a novel fusion partner of *MLL* in acute myeloid leukemia

Heiko Becker,<sup>1-3</sup> Gabriele Greve,<sup>1,2</sup> Keisuke Kataoka,<sup>4</sup> Jan-Philipp Mallm,<sup>5,6</sup> Jesús Duque-Afonso,<sup>1,2,7</sup> Tobias Ma,<sup>1,2</sup> Christoph Niemöller,<sup>1,2</sup> Milena Pantic,<sup>1</sup> Justus Duyster,<sup>1-3</sup> Michael L. Cleary,<sup>7</sup> Julia Schöler,<sup>8</sup> Karsten Rippe,<sup>5,6</sup> Seishi Ogawa,<sup>3</sup> and Michael Lübbert<sup>1-3</sup>

<sup>1</sup>Department of Medicine I, Medical Center, and <sup>2</sup>Faculty of Medicine, University of Freiburg, Freiburg, Germany; <sup>3</sup>German Cancer Consortium partner site, Freiburg, Germany; <sup>4</sup>Department of Pathology and Tumor Biology, Kyoto University, Kyoto, Japan; <sup>5</sup>Division of Chromatin Networks and <sup>6</sup>Single-cell Open Laboratory, German Cancer Research Center, Heidelberg, Germany; <sup>7</sup>Department of Pathology, Stanford University, Stanford, CA; and <sup>8</sup>Charles River Discovery Research Services Germany GmbH, Freiburg, Germany

## Key Points

- mRNA decapping gene *EDC4* is a novel fusion partner of *MLL* in AML.
- Genes functioning in mRNA decapping may compose a distinct group of *MLL* fusion partners that links *MLL* function with mRNA decapping in AML.

## Introduction

Translocations involving *MLL* (aka *KMT2A*) located on chromosome 11q23 occur in acute myeloid leukemia (AML) and lymphoblastic leukemia. In AML, they generally confer an adverse prognosis, unless the *MLL3* (aka *AF9*) gene is involved.<sup>1</sup> More than 130 different translocation partner genes (TPGs) have been identified, forming the *MLL* recombinome.<sup>2</sup>

Recently, the scavenger messenger RNA (mRNA) decapping enzyme DCPS has been identified to be required for survival of AML cells, but not normal hematopoietic cells, and a DCPS inhibitor showed antileukemic activity.<sup>3,4</sup> *DCPS* is also 1 of 2 genes (the other being *DCP1A*) involved in mRNA decapping and having been described as TPG of *MLL* in single leukemia cases.<sup>5-7</sup>

Here, we describe a novel *MLL* fusion with another mRNA decapping component, ie, the enhancer of mRNA decapping 4 gene (*EDC4*; also known as *GE1* or *HEDLS*), in AML. *EDC4* is part of a multiprotein complex in the cytoplasmic P bodies. It is required for the interaction of DCP2 and its cofactor DCP1 to remove the 5'-cap that is generated during transcription and crucial for protection from degradation.<sup>8,9</sup> As recently shown, *EDC4* has an additional, nuclear activity in DNA double strand break repair; its deficiency induces a phenotype comparable to BRCA1 deficiency.<sup>10</sup> Mutations in *EDC4* occur in various cancers, but rearrangements have not yet been described.<sup>11</sup>

## Methods

### Sample processing

Samples, collected at various time points as indicated in supplemental Figure 1, were enriched for mononuclear cells (MNCs) via Ficoll-Hypaque and depleted from CD3<sup>+</sup> cells via autoMACS (Miltenyi Biotec), as previously described.<sup>12</sup> CD3<sup>+</sup> cells served as germline control. The patient provided written informed consent for the research use of the clinical data and biomaterial in accordance to the Declaration of Helsinki.

### RNA sequencing

RNA sequencing libraries were prepared using the NEBNext Ultra RNA Library Prep Kit (New England Biolabs); sequencing was performed on a HiSeq 2500 system (Illumina). Fusion transcripts were detected by Genomon-fusion pipeline (<https://github.com/Genomon-Project/>), as previously described.<sup>13</sup> Reference transcript sequences were for *MLL* NM\_005933.1 and for *EDC4* NM\_014329.4. The primers used for polymerase chain reaction and sequencing of reverse-transcribed RNA had the following the sequences: *MLL*, ccagctggaaattggtgtt; *EDC4*, gatgatcctcgaaagtgtt.

## Animal model

NOD.Cg-Prkdc<sup>scid</sup>Il2rg<sup>tm1Sug</sup>/JicTac (NOG) were obtained from Taconic, Denmark. At 6 to 8 weeks of age, mice received  $3 \times 10^6$  primary blasts from peripheral blood to establish patient-derived xenograft (PDX) models. Cells were injected into the tibia, and animals were observed for clinical signs of leukemia (hind limb paresis, weight loss, bad overall condition). When moribund, mice were euthanized and human leukemic cells harvested from bone marrow (BM) and spleen. Subsequently,  $3 \times 10^6$  human leukemic cells were implanted into naive recipient mice. The study was carried out in accordance with the recommendations by the Society of Laboratory Animal Science. The animal experiments were approved by the regional council (Regierungspräsidium Freiburg, ref. 35, permit no. G-12/86).

## Exome sequencing

The SureSelect Human All Exon v5 Kit (Agilent Technologies) was used for exome capturing from genomic DNA, and sequencing was performed on a HiSeq 2500 system (Illumina). Sequence alignment and mutation calling were performed using the Genomon pipeline (<https://github.com/Genomon-Project/>), as previously described,<sup>13,14</sup> with minor modifications. Candidate mutations with (1) Fisher's exact test,  $P < .01$ ; and (2) a variant allele frequency in matched normal samples  $<0.2$  was adopted and further filtered by excluding (1) known variants listed in the 1000 Genomes Project (May 2011 release), NCBI dbSNP build 131, National Heart, Lung, and Blood Institute Exome Sequencing Project 5400, the Human Genome Variation Database (October 2013 release), or an in-house single-nucleotide polymorphism database; and (2) variants present in unidirectional reads only.

## Single-cell RNA sequencing

Single-cell RNA sequencing was performed on the MNC fraction of an available peripheral blood sample collected shortly before time point t2 using the chromium system (10X Genomics). Approximately 8000 cells were loaded on the chip, and library preparation was done according to the manufacturer's instructions. The library was sequenced on 1 lane 26+74 bp paired-end on a HiSeq4000 machine (Illumina). Reads were processed with cell ranger software using an annotation that contained protein coding genes only to yield a unique molecular identifier (UMI) count table that was then further processed with Seurat.<sup>15</sup> Low-quality cells were excluded from the analysis and regression was done using UMI count and cell-cycle stage. The normalized data were clustered using 7 PCA components as determined by an elbow plot. Marker genes were calculated by comparing a single cluster within the same cell type to all other clusters of the same cell type.

## Results and discussion

### Identification of *EDC4* as a fusion partner of *MLL*

A 55-year-old patient presented with a myelodysplastic syndrome (MDS; timepoint [t] -1) that progressed to AML (t0). The patient refused treatment beyond supportive care. Six months later, blast expansion occurred (t1). The patient received 5 courses of decitabine (t2), followed by 3 months of hydroxyurea (t3) (supplemental Figure 1). Cytogenetics at t0 revealed a previously undescribed translocation involving the chromosomal location of *MLL*: 46,XX,t(11;16)(q23;q12)[12]/46,XX[8]. The *MLL* rearrangement was detectable via interphase fluorescence in situ hybridization in 84 of 100 cells.

RNA sequencing identified the fusion partner to be *EDC4* on chromosome 16q22 (Figure 1A). The translocation led to the in-frame fusion of *MLL* exon 13 to *EDC4* exon 6, linked by 19 nucleotides of *EDC4* intron 5. The predicted amino acid sequence of this linker was ALNTLLR (Figure 1A). *MLL-EDC4* was present at diagnosis and during the course of the AML, but not during MDS (Figure 1B).

The *MLL-EDC4* protein has a predicted molecular weight of  $>200$  kD and contains most of *EDC4*, including the  $\alpha$ -helical domain at the C terminus, which mediates binding to DCP2 and the exonuclease XRN1. However, it lacks  $\sim 80\%$  of the WD40 domain of *EDC4*, which is required for the interaction with DCP1.<sup>9,16</sup>

*MLL-EDC4* stands out because of its fusion of *MLL* exon 13;  $<0.5\%$  of *MLL*-rearranged cases harbor a breakpoint in exon 13 or farther downstream.<sup>2</sup> However, as in most *MLL* rearrangements, the plant homology domain (PHD)/bromodomain (BD) function is likely impaired in *MLL-EDC4* (PHD1 and PHD2 are retained; PHD3, BD, and PHD4 are missing). An intact PHD/BD domain is critical for determining whether *MLL* acts as transcriptional activator or repressor; moreover, PHD2 and PHD3 are important for maintaining the stability of *MLL*.<sup>2</sup> Thus, the *MLL-EDC4* fusion could lead to perturbation of epigenetic gene regulation by *MLL*. Moreover, it is tempting to speculate that *MLL-EDC4* may lead to *EDC4* haploinsufficiency, as the heterozygous knockout of *EDC4* in a mouse model induces a myeloid phenotype featuring increased granulocyte counts.<sup>17</sup>

To study the potential oncogenic function of *MLL-EDC4*, we attempted to express it in mammalian cells; however, we were not able to successfully clone the full-length *MLL-EDC4* because of its high molecular weight. A truncated construct including only the conserved WD40 region of *EDC4* fused to *MLL* did not result in transformation of normal BM progenitor cells, whereas *MLL-AF9* and *E2A-PBX1* did (data not shown). Self-renewal capacity of the *MLL-EDC4*<sup>+</sup> AML could be demonstrated through serial transplantation using a PDX model established from primary patient blasts in NOG mice (Figure 1C).

### Identification of accompanying gene mutations and clonal evolution

To identify cooperating mutations and characterize clonal evolution, we performed exome sequencing. We identified a *STAG2* mutation as potential founder mutation during MDS (t1), which persisted throughout the disease course (Figure 1D). At the time of acquisition of *MLL-EDC4* (t1), 1 mutation each in *KRAS* (p.G13D) and *NRAS* (p.G12C) was detectable. Toward the terminal phase (t3), these mutations disappeared and a *FLT3* mutation (p.D835V) emerged (Figure 1D).

Mutations in *STAG2* impair sister chromatid cohesion after DNA replication and thereby segregation of chromosomes into daughter cells.<sup>18</sup> Aberrant chromosome segregation has also been associated with alterations in the splicing machinery,<sup>19</sup> and the recent report on DCPS function in AML indicated a direct link between mRNA decapping and splicing regulation.<sup>9</sup> Hence, one may speculate that it was the combined effect of mutated *STAG2* and *MLL-EDC4* on chromatid cohesion, splicing, and mRNA degradation that conferred a clonal advantage.

*NRAS* or *KRAS* mutations each occur in  $\sim 20\%$  and *FLT3* mutations in 10% to 15% of patients with *MLL*-rearranged AML.<sup>20</sup> Similar mutation patterns of *MLL-EDC4*<sup>+</sup> and other *MLL*-rearranged AMLs suggest that they share biological features. Of note, the previously

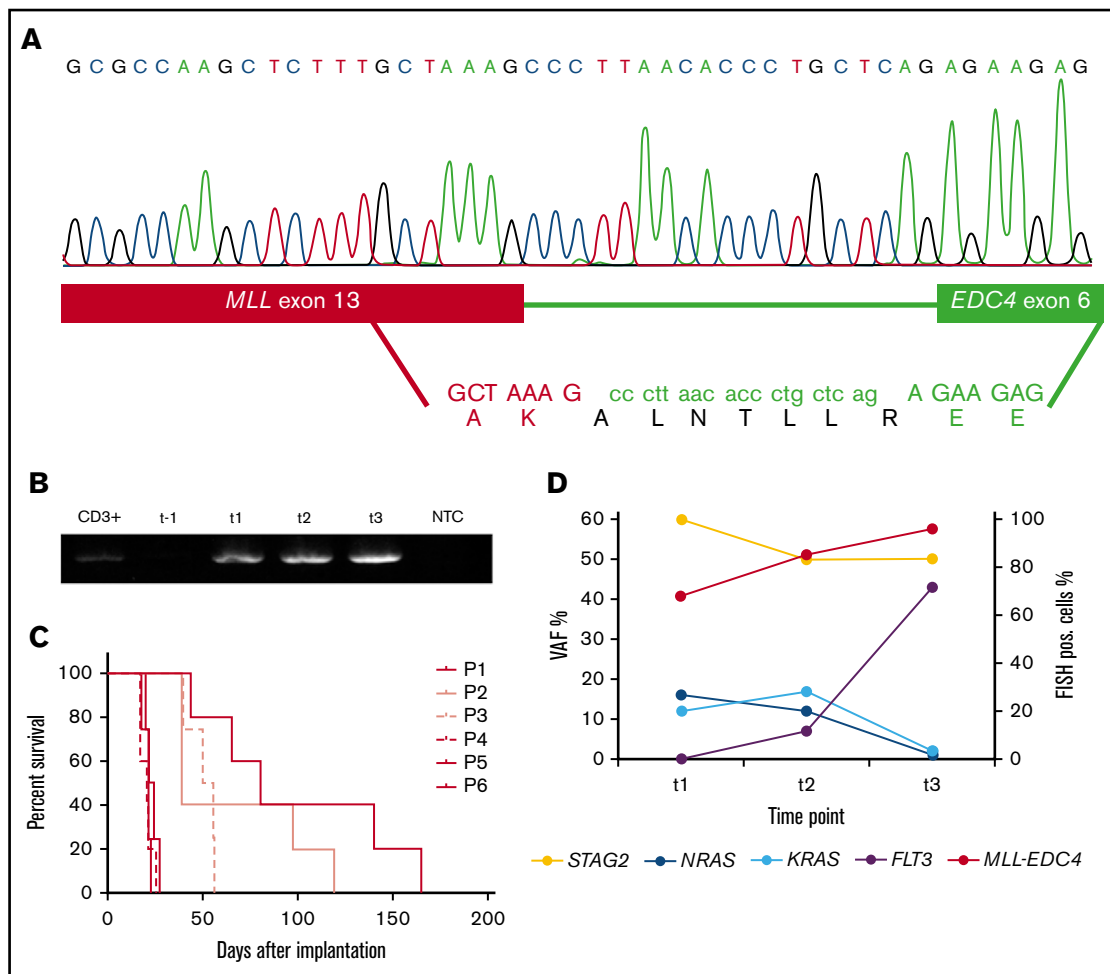


**Figure 1. Identification of the *MLL-EDC4* fusion and accompanying mutations.** (A) In-frame fusion of *MLL* exon 13 (red bar) to *EDC4* exon 6 (green bar) linked by 19 nucleotides from *EDC4* intron 5, resulting in the predicted amino acid sequence ALNTLLR inserted between *MLL* p.K1565 and *EDC4* p.E215. (B) Gel electrophoresis of the polymerase chain reaction on reverse-transcribed *MLL-EDC4* mRNA at the indicated time points. (C) Patient-derived xenograft model of the *MLL-EDC4*<sup>+</sup> AML. Survival of NOG mice after injection of primary patient blasts (P1) collected at t2 and after serial transplantation (P2-P6). (D) VAFs (derived from exome sequencing) of the mutations in *STAG2* (NM\_006603: c.463-1G>C), *NRAS* (p.G12C), *KRAS* (p.G13D), and *FLT3* (p.D835V) at t1, t2, and t3, displaying the presence of the *NRAS* and *KRAS* mutations before the start of decitabine and the increase of the *FLT3*-mutated clone toward t3. FISH, fluorescence in situ hybridization; NTC, no template control; P, passage; pos., positive; VAF, variant allele frequency.

described *MLL-DCPS*<sup>+</sup> AML harbored no mutations in *FLT3* or *NRAS* (K. H. Metzeler, Ludwig-Maximilians University, Munich, Germany, written communication, 12 October 2018).<sup>4</sup>

### Characterization of the phenotype of the *MLL-EDC4*<sup>+</sup> AML

As assessed by flow cytometry of the BM, the blasts at t0 were CD117<sup>+</sup> with partial coexpression of CD33 (65%), CD34 (65%) and MPO (20%).

To further characterize the phenotype associated with *MLL-EDC4*, we performed single-cell RNA sequencing on CD3<sup>+</sup> cell-depleted MNCs. Of the cells, 86% were identified to be leukemic blasts. The remaining cells were monocytes or residual erythroblasts (Figure 2A). Focusing on a set of candidate genes with potential biological relevance,<sup>21,22</sup> the blasts featured strong coexpression of *MYB*, *HOXA9*, and *HOXA10* and lower expression of *EDC4*, *HOXA4*, and *HOXA5*. In contrast, *HOXB5*, *HOXB6* and *HOXC4* were not detected (Figure 2B). Because one consequence of

*MLL-EDC4* could be impaired DNA repair resulting from *EDC4* deficiency,<sup>10</sup> it appears noteworthy that the AML displayed marked upregulation of *PARP1* and genes of the MRN complex (ie, *MRE11*, *RAD50*, and *NBN*) (data not shown).

We next determined clusters of cells based on the differences in gene expression (clusters 0-7) and identified marker genes for a given cluster (supplemental Figure 2). These analyses confirmed the phenotypical heterogeneity among the leukemic blasts and identified the transcription factor *HEMGN* (aka *EDAG*, which regulates myelopoiesis)<sup>23</sup> and the GTPase *GIMAP7* to be enriched among CD34<sup>+</sup> cells.

In conclusion, the fusion of *MLL* with *EDC4* characterized here complements the recently established role of mRNA decapping in AML. In conjunction with the previously described *MLL* fusions to *DCP1A* and *DCPS*, our findings raise the possibility that mRNA decapping enzymes compose a distinct group of recurrent TPGs of *MLL*, emphasizing a possible link between *MLL* functions and mRNA decapping. In our case, *MLL-EDC4* likely cooperated

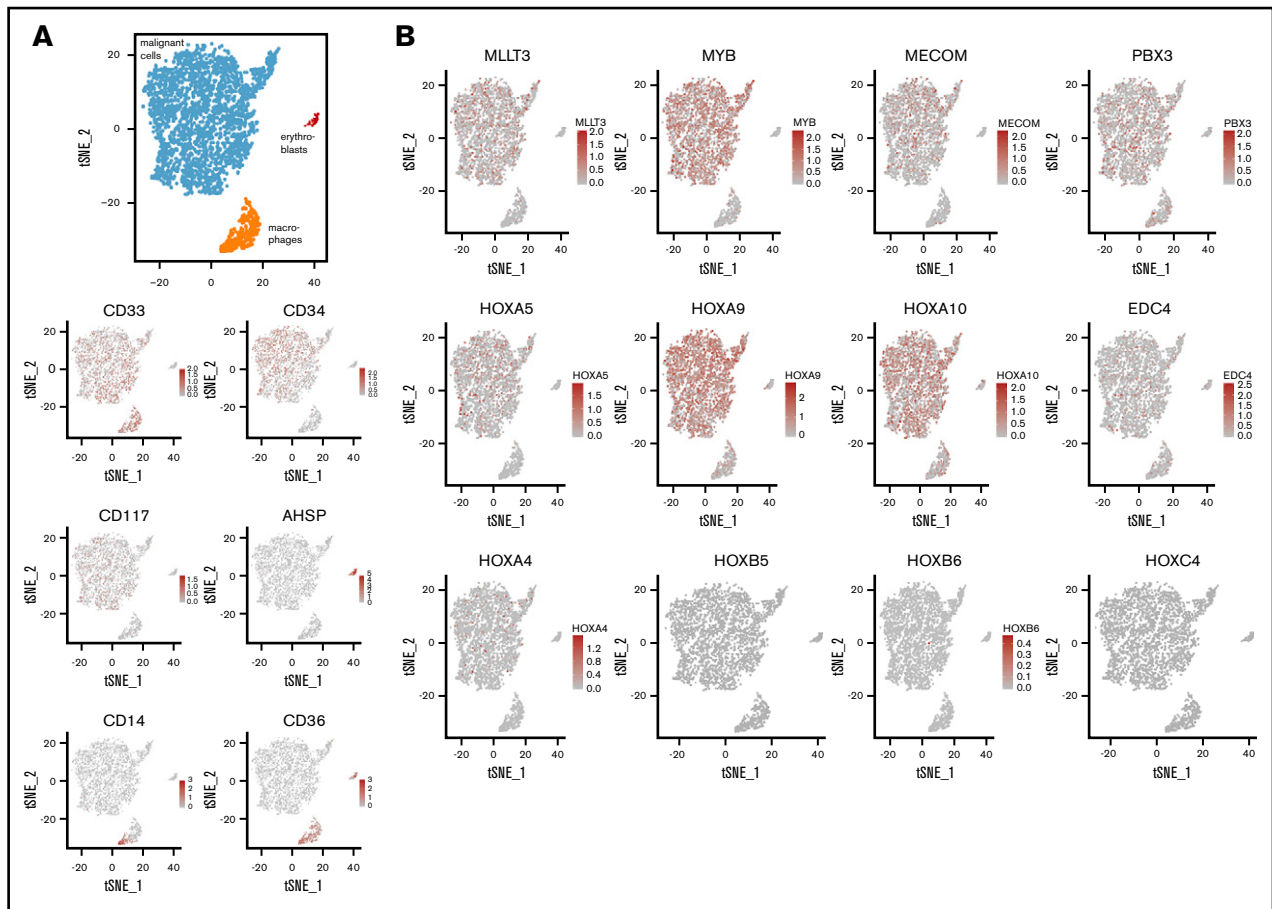


**Figure 2. Single-cell RNA expression analysis.** (A) tSNE plot with coloring according to cell type as determined by marker gene expression and as depicted in the heatmaps. Expression level is provided as UMI counts. (B) Expression of selected genes across all cells. tSNE, t-distributed stochastic neighbor embedding.

with aberrant chromatid cohesion and proliferation signaling; self-renewal capacity was demonstrated in a PDX model.

## Acknowledgments

The authors thank J. Surrallés Calonge (Universitat Autònoma de Barcelona, Bellaterra, Spain) for insightful discussions on EDC4, and C. Meyer (University of Frankfurt, Frankfurt, Germany) and K. H. Metzeler (Ludwig-Maximilians University, Munich, Germany) for background information on the *MLL-DCPS* positive AML case.

This research was supported by the Translational Research Training in Hematology of the European Hematology Association and American Society of Hematology (H.B.); the German Research Foundation (SPP 1463 LU 429/8-2 [M.L.]; CRC992 MEDEP C04 [M.L.]; FOR 2674 BE 6461/1-1 [H.B.], LU 429/16-1 [M.L.], MA 7792/1-1 [J.-P.M.], RI 1283/15-1 [K.R.]; and DU 1287/2-1 [J.D.-A.]; and German Cancer Aid (111210) (H.B.).

## Authorship

Contribution: H.B. undertook conception and design; patient care; specimen acquisition; data acquisition, analyses, and interpretation; analysis coordination; and manuscript preparation; G.G. undertook specimen processing; data acquisition, analyses, and interpretation; and analysis coordination; K.K. provided RNA sequencing and exome sequencing data acquisition, analyses, and interpretation;

J.-P.M. managed single-cell RNA sequencing data acquisition, analyses, and interpretation; J.D.-A. undertook data acquisition, analyses, and interpretation; T.M. provided specimen processing, data acquisition and analyses, and analysis coordination; C.N. managed specimen processing, data acquisition, and analyses; M.P. managed fluorescence in situ hybridization data acquisition, analyses, and interpretation; J.D. undertook conception and design and data interpretation; M.L.C. undertook conception and design and data interpretation; J.S. provided patient-derived xenograft model generation, and data analyses and interpretation; K.R. managed single-cell RNA sequencing experimental design and interpretation; S.O. undertook RNA sequencing and exome sequencing data acquisition, analyses, and interpretation; and M.L. undertook conception and design; patient care; specimen acquisition; data acquisition, analyses, and interpretation; analysis coordination; and manuscript preparation.

Conflict-of-interest disclosure: The authors declare no competing financial interests.

ORCID profiles: H.B., 0000-0002-6919-4048; K.K., 0000-0002-8263-9902.

Correspondence: Michael Lübbert, Department of Medicine I, Medical Center, University of Freiburg, Hugstetter Str 55, 79106 Freiburg, Germany; e-mail: michael.luebbert@uniklinik-freiburg.de.

## References

1. Döhner H, Estey E, Grimwade D, et al. Diagnosis and management of AML in adults: 2017 ELN recommendations from an international expert panel. *Blood*. 2017;129(4):424-447.
2. Meyer C, Burmeister T, Gröger D, et al. The MLL recombinome of acute leukemias in 2017. *Leukemia*. 2018;32(2):273-284.
3. Yamauchi T, Masuda T, Carver MC, et al. Genome-wide CRISPR-Cas9 screen identifies leukemia-specific dependence on a pre-mRNA metabolic pathway regulated by DCPS. *Cancer Cell*. 2018;33(3):386-400.
4. Taverniti V, Séraphin B. Elimination of cap structures generated by mRNA decay involves the new scavenger mRNA decapping enzyme Aph1/FHIT together with DcpS. *Nucleic Acids Res*. 2015;43(1):482-492.
5. Meyer C, Schneider B, Reichel M, et al. Diagnostic tool for the identification of MLL rearrangements including unknown partner genes. *Proc Natl Acad Sci USA*. 2005;102(2):449-454.
6. Meyer C, Kowarz E, Hofmann J, et al. New insights to the MLL recombinome of acute leukemias. *Leukemia*. 2009;23(8):1490-1499.
7. Krumbholz M, Bradtke J, Stachel D, et al. From initiation to eradication: the lifespan of an MLL-rearranged therapy-related paediatric AML. *Bone Marrow Transplant*. 2015;50(10):1382-1384.
8. Arribas-Layton M, Wu D, Lykke-Andersen J, Song H. Structural and functional control of the eukaryotic mRNA decapping machinery. *Biochim Biophys Acta*. 2013;1829(6-7):580-589.
9. Chang CT, Bercovich N, Loh B, Jonas S, Izaurralde E. The activation of the decapping enzyme DCP2 by DCP1 occurs on the EDC4 scaffold and involves a conserved loop in DCP1. *Nucleic Acids Res*. 2014;42(8):5217-5233.
10. Hernández G, Ramírez MJ, Minguillón J, et al. Decapping protein EDC4 regulates DNA repair and phenocopies BRCA1. *Nat Commun*. 2018; 9(1):967.
11. Forbes SA, Bindal N, Bamford S, et al. COSMIC: mining complete cancer genomes in the Catalogue of Somatic Mutations in Cancer. *Nucleic Acids Res*. 2011;39(Database issue):D945-D950. <https://doi.org/10.1093/nar/gkq929> <http://www.sanger.ac.uk/cosmic>. Accessed 24 June 2018
12. Stosch JM, Heumüller A, Niemöller C, et al. Gene mutations and clonal architecture in myelodysplastic syndromes and changes upon progression to acute myeloid leukaemia and under treatment. *Br J Haematol*. 2018;182(6):830-842.
13. Kataoka K, Nagata Y, Kitanaka A, et al. Integrated molecular analysis of adult T cell leukemia/lymphoma. *Nat Genet*. 2015;47(11): 1304-1315.
14. Becker H, Yoshida K, Blagitko-Dorfs N, et al. Tracing the development of acute myeloid leukemia in CBL syndrome. *Blood*. 2014;123(12): 1883-1886.
15. Butler A, Hoffman P, Smibert P, Papalexi E, Satija R. Integrating single-cell transcriptomic data across different conditions, technologies, and species. *Nat Biotechnol*. 2018;36(5):411-420.
16. Braun JE, Truffault V, Boland A, et al. A direct interaction between DCP1 and XRN1 couples mRNA decapping to 5' exonucleolytic degradation. *Nat Struct Mol Biol*. 2012;19(12):1324-1331.
17. Smith CL, Blake JA, Kadin JA, Richardson JE, Bult CJ; the Mouse Genome Database Group. 2018. Mouse Genome Database (MGD)-2018: knowledgebase for the laboratory mouse. *Nucleic Acids Res*. 2018;46(D1):D836-D842.
18. Solomon DA, Kim T, Diaz-Martinez LA, et al. Mutational inactivation of STAG2 causes aneuploidy in human cancer. *Science*. 2011;333(6045): 1039-1043.
19. Sundaramoorthy S, Vázquez-Novelle MD, Lekomtsev S, Howell M, Petronczki M. Functional genomics identifies a requirement of pre-mRNA splicing factors for sister chromatid cohesion. *EMBO J*. 2014;33(22):2623-2642.
20. Grossmann V, Schnittger S, Poetzinger F, et al. High incidence of RAS signalling pathway mutations in MLL-rearranged acute myeloid leukemia. *Leukemia*. 2013;27(9):1933-1936.
21. Lee S, Chen J, Zhou G, et al. Gene expression profiles in acute myeloid leukemia with common translocations using SAGE. *Proc Natl Acad Sci USA*. 2006;103(4):1030-1035.
22. Alharbi RA, Pettengell R, Pandha HS, Morgan R. The role of HOX genes in normal hematopoiesis and acute leukemia. *Leukemia*. 2013;27(5): 1000-1008.
23. Li CY, Zhan YQ, Li W, et al. Overexpression of a hematopoietic transcriptional regulator EDAG induces myelopoiesis and suppresses lymphopoiesis in transgenic mice. *Leukemia*. 2007;21(11):2277-2286.